The MAPP Outrigger Technical Proposal

Version 1.0 - 6th June 2023
The MoEDAL-MAPP Collaboration

B. Acharya[1,2] J. Alexandre[1] P. Benes[3] B. Bergmann[3] A. Bevan[4] H. Branzas[5] P. Burian[3] M. Campbell[6] S Cecchini[7] Y. M. Cho[8] M. de Montigny[9] M. de Montigny[9] A. de Roeck[6] J. Ellis[1] M. Fairbairn[1] D. Felea[5] M. Frank[10] J. Hays[4] A. M. Hirt P.Q. Hung[12] J. Janecek[3] M. Kalliokoski[13] D. Lacarèrre[6] C. Leroy[14] G. Levi[7] J. Mamuzik[15] A. Maulik[7,9] A. Margiotta[7,16] N. Mauri[7] N. E.Mavromatos[1,17] N. E.Mavromatos[1,17] M. Mieskolainen[18] L. Millward[4] V. A. Mitsou[15] G. Moss[19] I. Ostrovskiy[20] P.-P. Ouimet[21] J. Papavassilou[15] L. Patrizii[7] G. E. Păvălaş[5] J. L. Pinfold[9,1] L. A. Popa[5] V. Popa[5] M. Pozzato[7] S. Pospisil[3] S. Pospisil[3] A. Rajantie[21] R. Ruiz de Austi[15] A. Salazar Lobos[9] Z. Sahnoun[7,23] M. Sakellariadou[1] S. Sarkar[1] G. Semenoff[24] A. Shaa[9] G. Sirri[7] K. Sliwa[7] R. Soluk[9] M. Spurio[7] M. Staelens[9] M. Suk[3] M. Tenti[25] V. Togo[7] J. A. Tuszynski[9] A. Upreti[20] V. Vento[7] O.Vives[7]

[1*]Theoretical Particle Physics & Cosmology Group, King's College London, UK.
[2*]International Centre for Theoretical Physics, Trieste, Italy .
[3]IEAP, Czech Technical University in Prague, Czech Republic .
[4]School of Physics and Astronomy, Queen Mary University of London, London, England .
[5]Institute of Space Science, Bucharest - Măgurele, Romania .
[6]Experimental Physics Department, CERN, Geneva, Switzerland .
[7]INFN, Section of Bologna, Bologna, Italy .
[8]Asia Pacific Center for Theoretical Physics, Pohang, Korea .
[9]Physics Dept., University of Alberta, Edmonton, Alberta, Canada .
[10]Dept. of Physics, Concordia University, Montréal, Quebec, Canada .
[11]Dept. of Earth Sciences, Swiss Federal Institute of Technology, Zurich, Switzerland .
[12]Dept. of Physics, University of Virginia, Charlottesville, Virginia, USA .
[13]Physics Dept., University of Helsinki, Helsinki, Finland .
[14]Department of Physics, Concordia University, Montréal, Quebec, Canada .
[15]IFIC, Universitat de Valéncia - CSIC, Valéncia, Spain .
[16]Department of Physics & Astronomy, University of Bologna, Italy .
[17]National Technical University of Athens, Zografou Campus, Athen, Greece .
[18]Physics Dept., University of Helsinki, Helsinki, Finland .
[19]Track Analysis Systems Ltd, Bristol, UK .
[20]Physics Department, University of Alabama, Tuscaloosa, Alabama, USA .
[21]Physics Department, University of Regina, Regina, Saskatchewan .
[22]Physics Department, University of Regina, Regina, Saskatchewan .
[23]Centre for Astronomy, Astrophysics and Geophysics, Algiers, Algeria .
[24]Department of Physics, UBC, Vancouver, British Columbia, Canada .
[25]INFN, CNAF, Bologna, Italy
.
[*]**Communicating Author, E-mail: jpinfold@ualberta.ca** .

Abstract

This is the Technical Proposal for the Outrigger Detector for the MAPP-1 (moEDAL Apparatus for Penetrating Particles) detector currently being installed in UA83 for data taking during LHC's Run-3. The Outrigger is an auxiliary detector designed to greatly improve the acceptance of the Phase-1 MAPP detector (MAPP-1) for mini-charged particles with larger fractional charges. The Outrigger Detector is comprised of four 6m scintillator planks, comprised of 60 cm x 30 cm x 5 cm scintillator slabs, deployed in three horizontal shafts joining the UA83 tunnel to the beam tunnel in the vicinity of the MAPP detector.

1 Introduction

A major part of the MoEDAL Collaboration's physics program for LHC's Run-3 and beyond involves the installation of a new detector called MAPP-1 (MoEDAL Apparatus for Penetrating Particles) [1]. MAPP's purpose is to expand the physics reach of MoEDAL, that is focussed on the detection of Highly Ionizing Particle (HIP) avatars of new physics, to include the search for mini-charged particles[1] (mCPs) with charges as low as one thousandth the electron charge (e) and weakly interacting very long-lived neutral particle (LLPs) messengers of new physics. Thus the MoEDAL and MAPP detectors operating together will be able to detect: HIPs, mCPs and LLPs.

The MAPP-1 outrigger detector is an array of scintillator blocks arranged in planks placed in three ducts joining the UA83 tunnel and the beamline tunnel, in the vicinity of the MAPP detector, as indicated in Figure 1. Its purpose is to significantly increase MAPP's acceptance for feebly electromagnetically interacting particles with an effective charge greater than $\sim 0.01e$, where e is a single electric charge. This Technical Proposal describes the details of the design, construction and installation of the "Outrigger Detector."

2 The Outrigger Detectors for the MAPP Phase-1 Detector

The Phase-1 MAPP detector (MAPP-1) for LHC's Run-3 is currently being installed in UA83 tunnel some 100 m from the existing MoEDAL & LHCb detectors, in order to take data during LHC's Run-3. The MAPP-1 detector and its associated electronics rack has now been included in the overall LHC machine description as shown in Figure 1. A drawing of the MAPP-1 detector is shown in Figure 2. MAPP-1 is protected from Standard Model particles from interactions at IP8 by roughly 35m to 40m of rock and from cosmic rays by an overburden of approximately 110m of limestone.

[1] We use the term mini-charged rather than milli-charged to denote the lightly ionizing particle as it does not imply that the charge is $10^{-3}e$

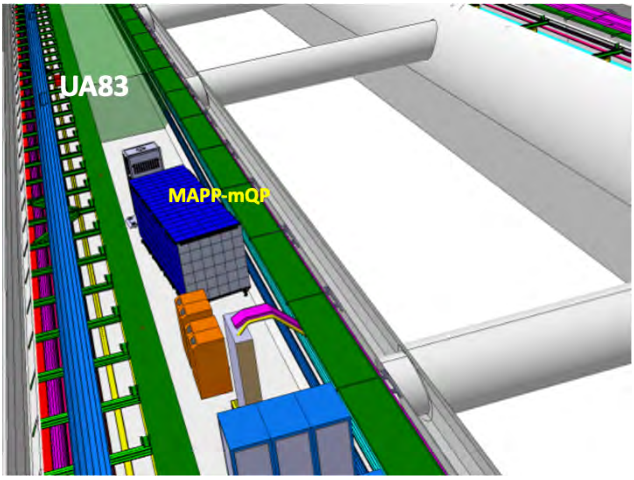

(a)

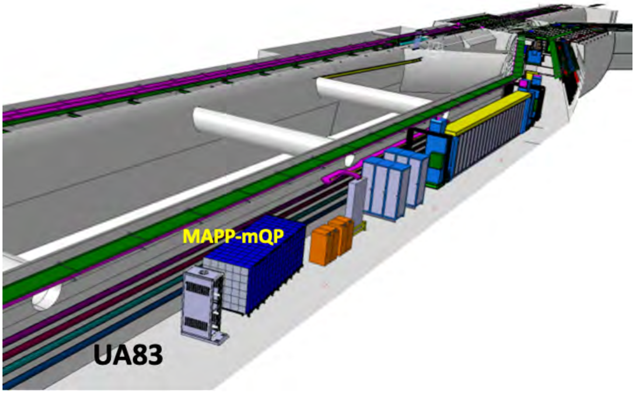

(b)

Fig. 1: The deployment of the MAPP-mQP detector in UA83.

The MAPP Phase-1 detector is designed to the search for mCPs. It is made up of four collinear sections, with sensitive cross-sectional area of roughly 1.0 m^2, each comprised of 100 (10 cm $\times$ 10 cm) plastic scintillator bars each 75cm long. Each bar is readout by one low-noise 3-inch PMT. The detector is arranged to point toward the IP. Thus, each through-going particle from the IP will encounter 3.0 m of scintillator and be registered by a coincidence of 4 PMTs. The 4-fold PMT coincidence essentially eliminates the background from "dark counts" in the PMTs. Additionally, the division of the detector into 4 bars virtually excludes all fake 4-fold coincidences due to radiogenic

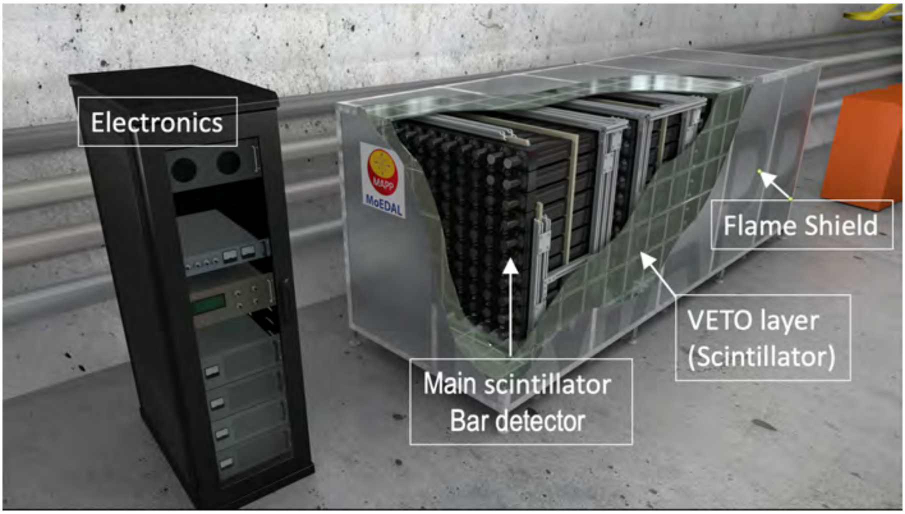

Fig. 2: A drawing of the MAPP detector showing the main elements of the MAPP detector.

backgrounds in the scintillator and PMTs. The MAPP-mCP "bar" detector is hermetically enclosed in a veto layer consisting of a 1 cm thick scintillator read out by embedded scintillating fibre loops with a 25 cm x 25 cm pitch.

The MAPP-1 Outrigger Detectors are placed adjacent to the MAPP-1 detector in three ducts joining the beamline tunnel to the UA83 tunnel, as shown in Figure 3. As shown in Figure 4 the outrigger detectors cover the region between 1.7° and 5.3° at a distance of 108.5m to 135.3m from IP8.

2.1 Outrigger Detector Technology

The basic scintillator unit of the Outrigger Detector is described in Figure 5. It is comprised a block of acrylic scintillator (Bicron BC-412) of size 60 cm x 30 cm x 5 cm readout through a light guide by a single 3.5-inch low noise PMT (HZC Photonics XP82B2FNB) [2] This unit is assembled on a frame with another unit for insertion on a rail into the shafts that house the Outrigger Detectors. This subdivision is chosen to facilitate manual handling. The units are held at an angle of 45° in order that the path length of particles from the IP in the scintillator is increased from 5cm to approximately 7 cm.

These scintillator subunits are installed in ducts 3, 4 and 5 joining the UA83 tunnel to the beam tunnel. The numbering of shafts starts from the end of UA83 nearest to IP8. Two scintillator layers are inserted in shaft 3 and one scintillator layer is inserted in ducts 4 and 5, as shown in Figure 6 and Figure 7. For example, a requirement for a gold-plated milli-charged particle candidate would be the coincidence of all 4 layers where the scintillator

[2] The HZC Photonics PMT is functionally the same as the HZC XP82B20D [2]

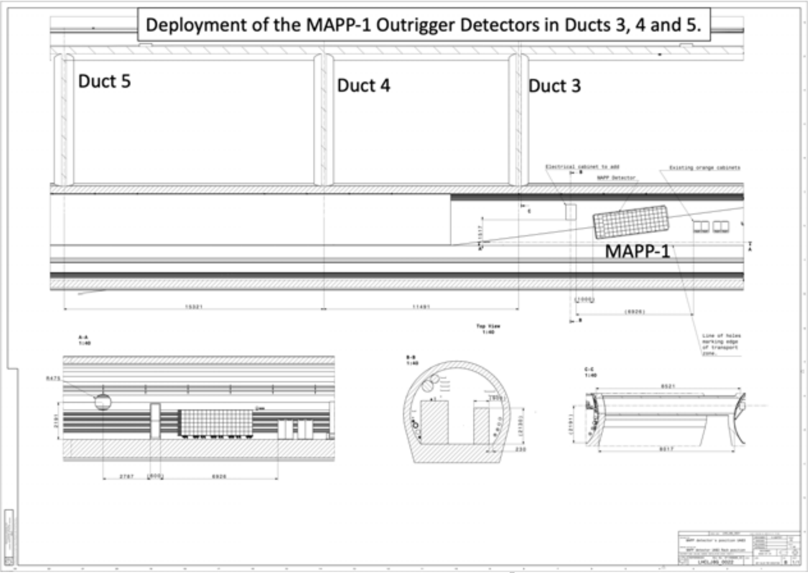

Fig. 3: The deployment of the Outrigger Detectors adjacent to the MAPP-1 detector.

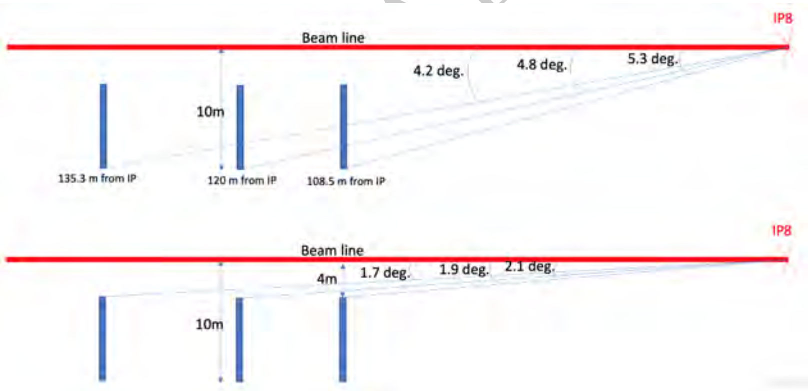

Fig. 4: The angular coverage of the Outrigger Detectors.

blocks responding would be those consistent with a track passing through the Outrigger Detectors.

Typically, a Minimum ionizing particle will lose around 2 MeV/cm in a good plastic scintillator and generate of the order of 10K to 20K photons per MeV lost. Consequently, this particle will deposit a comparatively large amount of light, of the order 1.4 x 10^5 photons in each scintillator block through which the muon passes. We have estimated that the light collection efficiency, including the loss due to photo-cathode efficiency, is 10%.

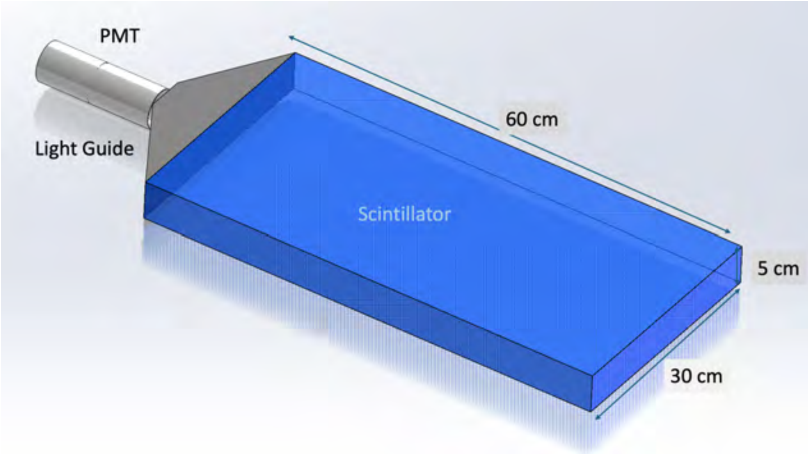

Fig. 5: The basic 5 cm thick plastic scintillator (Bicron 412) unit of the Outrigger Detector readout by a single 3.5-inch HZC Photonics (XP82B2FNB) PMT.

Roughly, a relativistic charged particle ionizes according to the square of its charge a particle with around $10^{-2}e$ would give approximately 14 photons in each bar. Assuming a quantum efficiency of 20% for the detecting PMT and a 50% efficiency for the photon reaching the PMT we should get of the order of one (PE). Thus, using this very approximate calculation the blocks are limited to the measurement of mCPs with a charge ofo $10^{-2}e$ and above.

However, number of other factors need to be taken in account including a detailed knowledge of the photon detection efficiency of each bar as well as factors that effect the particle by particle emission of scintillation light that depends on such factors as the charge, the velocity and Landau-Vavilov fluctuations [4] in energy loss. Indeed, at the limit of the sensitivity of the detector the most probable energy loss instead of the average energy loss is required.

A detailed simulation dealing with all of the above mentioned details is required especially when for small enough values of fractional charge the expected number of photons produced per MCP passing through the detector is less than one, pushing the limitations of the outrigger detector. Such as simulation named SUMMA (Simulation of the UA83, MoEDAL, MAPP-mCP Arena) has been created and is under test.

2.2 HV, Readout, DAQ, Calibration and Trigger

The PMT used in the readout of the scintillator bars is a HZC Photonics P82B2FNB PMT Tube. The High Voltage divider will be resistive with an impedance of 4MΩ a maximum voltage of 2000V and a current of 500μ A. The photocathode will be at ground potential with positive high voltage applied to the anode. The signal will be capacitively coupled to the cable.

The power supply will consist of a boost converter to convert from 48Vdc to 250V using a coupled inductor to reduce the maximum voltage seen by the controller. Several stages of a Cockcroft-Walton multiplier will then increase this up to 2000V. The boost converter will be controlled by a small inexpensive 6 pin micro-controller which can accept serial data and synchronization pulses from the DAQ The Front end is connected to the DAQ via an MCX connector. Power, signal and control will all be delivered via the same cable to reduce cabling costs. In this way we avoid HV cables and connectors as well as the related safety concerns

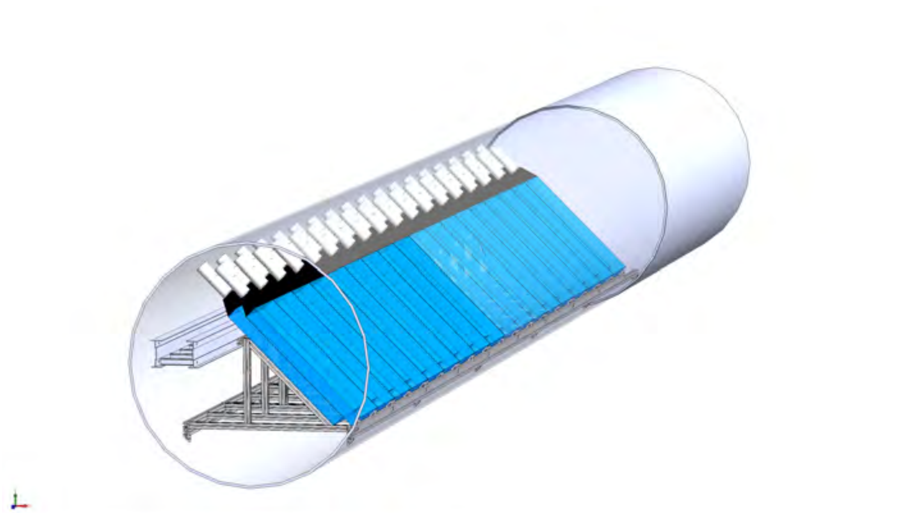

Fig. 6: The deployment of the outrigger detector in Shaft 3.

The technology for HV, readout, DAQ, calibration, and trigger used for the main MAPP-1 detector will also be used for the Outrigger Detector. However, the Outrigger will have its own software trigger and operate autonomously, although the data will use the same DAQ computers and data-path out of the cavern

A block diagram of the electronic readout and powering scheme for the MAPP and Outrigger Detectors is shown in Figure 8. Each DAQ board will consist of 32 identical channels. The DAQ will connect to the front end via an MCX connector. A bias tee will couple the 48V dc supply to the signal line. Control signals for the high-voltage power supply will also be coupled capacitively to the signal line. The amplifier will chain will include a programmable gain amplifier to allow tuning of the overall system gain, minimal shaping and an anti-alias filter. The ADC will consist of a Texas Instruments ADS4249 dual channel amplifier running at 240MHz, and a 14bit readout to an Intel (formally Altera) Cyclone IV FPGA via LVDS.

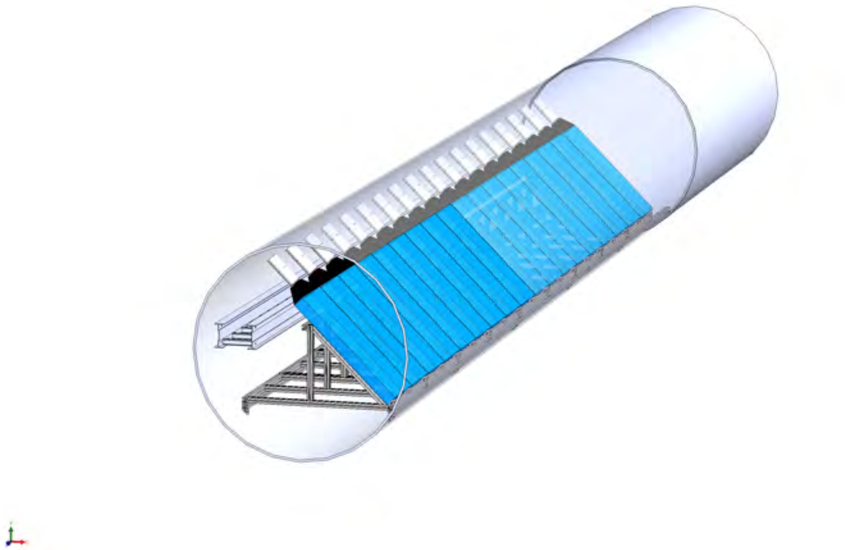

Fig. 7: The deployment of the Outrigger Detector in Shafts 4 and 5.

The FPGA will perform discrimination, coincidence and peak detection of the incoming signals, with inter-FPGA communication via backplane B-LVDS. Events that pass both the software trigger and the veto will be passed for storage via Ethernet to the PC(s). The system will run synchronously to the LHC (bunch crossing) clock, The orbit clock will also veto background events from non-colliding bunches and to synchronize health-keeping events and switching regulator noise to the abort gap.

Normally the data will be transferred via 1 Gbit/s ethernet link to an external computer. There will also be a computer in UGC1 that will take data if there is a failure in the ethernet connection. The data will be sent via the onsite storage via the internet to analysis sites in Canada, UK, USA, Spain and Italy. The 19 readout boards will be housed directly underneath the MAPP-mQP detector, in the UGC1 gallery.

The data rate is expected to be on average less than 1 Hz from each of the 400 bars of the MAPP main detector with around another 200 channels from the veto detectors and radiator at maximum. There are 80 extra channels contributed by the Outrigger Detector, corresponding to the 80 scintillator blocks comprising the detector.

Conservatively assuming a rate of, on average, 1 Hz for each of the 680 channels involved, with 200 bits per channel (or PMT pulse) being read out, the total data rate is around 140 Kbits/sec. Our system has the capacity to read out 4 million channels/s, 5900 times more capacity than needed. The data in the front end readout electronics is pipe-lined so that large fluctuations up

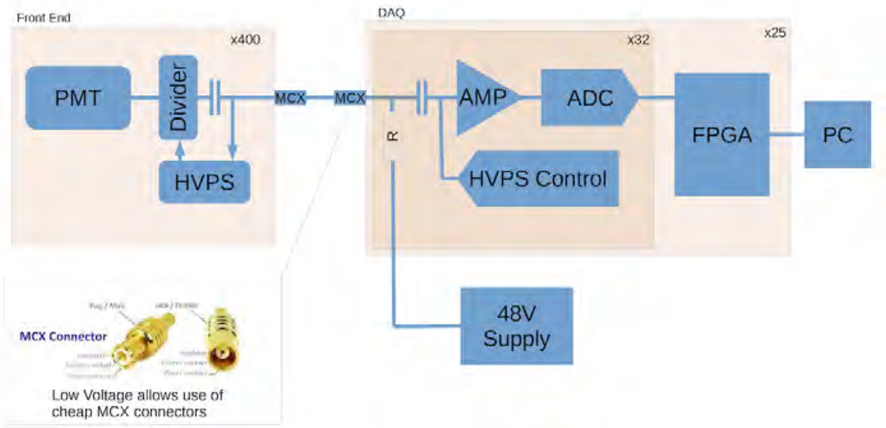

Fig. 8: A block diagram showing the basic electronics readout structure for the MAPP-mQP detector,

in the data rate can be handled. Thus, these boards could be used for high luminosity LHC.

There will be a number of software triggers carried out by FPGAs housed in the readout system. The trigger philosophy is to widen the trigger as much as possible. Additionally, we aim to take minimum bias events at the rate of approximately 5% of the total data rate. Nevertheless, we expect the amount of data readout will be somewhat less than the maximum mentioned just above. Further, higher-level "triggers', will be applied offline to the raw data. We chose to adopt the philosophy of utilizing a very broad software trigger, rather than reading out the complete detector at each beam crossing since the flow of data through the various triggers enables us to monitor the physics response of our detector online.

An example of an important "software" trigger for MAPP-1 and the Outrigger Detectors, is the through going muon-trigger. In this case the muon would pass through all four scintillator blocks pointing at the IP as well as the photon tagging boards (that can also serve as VETO detectors) that sandwich the main scintillator detector sections. In the MAPP-1 case a basic muon trigger is formed from a coincidence of 4 contiguous scintillator sections.

In the case of the Outrigger Detector, the muon trigger is formed by a "hit" in each of the four scintillator layers where those hits are consistent with forming a collinear track. In the case of the Outrigger detector the trigger efficiency of a through going muon is on average around 80%, rather that the essentially 100% expected for the MAPP-1 bar detector. This is because MAPP-1 has been designed as a pointing detector, whereas the Outrigger is only approximately pointing due to the nature of its required positioning.

The efficiency trigger efficiency to be very near 100%.

2.2.1 The Outrigger Detector Calibration System

Like the MAPP-1 detector, the Outrigger Detector will be calibrated in two main ways. The first method utilizes an array of blue LED's emitting at the peak of the wavelength sensitivity of the scintillator blocks forming the Outrigger Detector. Each scintillator block is equipped with a LED which is pulsed in such a way as to mimic the light deposited by particles with varying fractional charge, down to the level where only single photoelectrons are being detected by the PMTs.

The second calibration method employs the small flux of high-momentum muons from IP8. Characteristically, these muons will be minimum ionizing particles (MIPs). We can simulate the light emission of a fractionally charged particle by inserting a neutral density filter between the PMT and the scintillator block. The transmittance of the filter would be chosen to reduce the amount of light entering the PMT from the muon by the same amount that a fractionally charged particle would have reduced ionization compared to a MIP. This "absolute" calibration is transferred to the LED system by comparison of the signal generated by the calibration LED in the PMT to the signal obtained when a neutral density filter is interposed.

3 Beam Induced Radiation Backgrounds in the MAPP-1 Outrigger Detector Region of the UA83 Tunnel

A prototype MAPP-mQP detector was deployed in 2018. Its main purpose was to enable us to estimate the data rate we would expect during RUN-3. The prototype was comprised of nine 10 cm x 10 cm x 120 cm scintillator bars deployed in a *horizontal* configuration in the UGC1 gallery. Each bar was read out at both ends by a PMT. A hit on a scintillator bar was counted if the PMTs at each end of the bar registered a coincident signal above the threshold. We observed that with beam-off each bar was hit at around a rate $\sim$0.05 Hz. This rate was largely due to cosmic rays, despite the roughly 110m rock overburden. This level of the cosmic background was consistent with our GEANT-4 based simulations. We expect this level of cosmic ray activity in the UA83 tunnel as it lies at the same depth beneath the same rock overburden.

When the beam was turned on we observed the rate in the MAPP-mQP prototype bars increased by a factor of 4 to 5. According to the FLUKA studies presented in the above subsection on beam-induced radiation backgrounds in the MAPP-mCP region of the UA83 tunnel, the beam-induced backgrounds in the MAPP-mCP detector in UA83 should be considerably less than expected in UGC1, except in the regions where the ducts connect UA83 with the beam tunnel.

In order to study beam-induced backgrounds more fully Francesco Cerutti and Alessia Ciccotelli of the beam-Machine Interaction section of the CERN

Engineering Department has performed a study of the beam-induced backgrounds in the UA83 tunnel and the UGC1 gallery using the FLUKA Monte Carlo program, assuming an annual luminosity of 10 fb^{-1}.

A critical issue is the effect of the radiation on the detector and on its electronic readout system. A key variable here is the dose which is shown in Figure 9. As can be seen from Figure 9 the dose received by the MAPP-1 detector in its new position in the UA83 tunnel is estimated to be below 1mGy/year, a factor of 300 less than its initially proposed deployment in the UGC1 gallery.

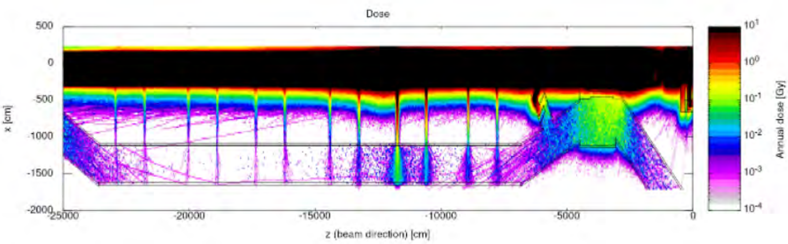

Fig. 9: The dose rate in the vicinity of MAPP-1. The top map shows the UGC1 gallery and the bottom map shows the UA83 tunnel.

Figure 10 depicts a map of the muon fluence component of beam-induced backgrounds expected at the UA83 ($< 10^6$ cm^{-2}) and UGC1 ($\sim 3 \times 10^8$ cm^{-2}) locations of the MAPP-mCP detector. We see a better than a 300 times reduction of the muon flux in the UA83 location compared to the UGC1 position.

Likewise the neutron flux (5×10^7/year) and photon flux (10^8 cm^{-2}/year) at the position of the MAPP-1 detector in UA83 show at least a few hundred times reduction over MAPP-1's previously proposed position in the UGC1 gallery, as laid out in Figure 11 and Figure 12, respectively.

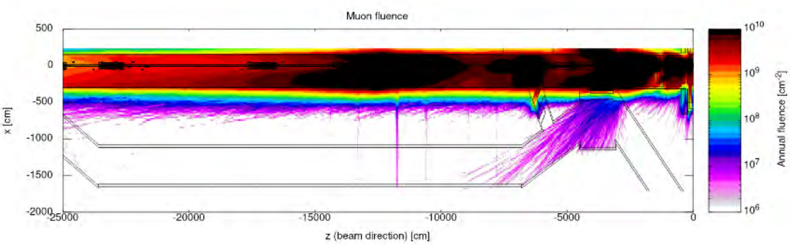

Fig. 10: The muon fluence in the vicinity of MAPP-1. The top part of map shows the UGC1 gallery and the bottom map shows the UA83 tunnel.

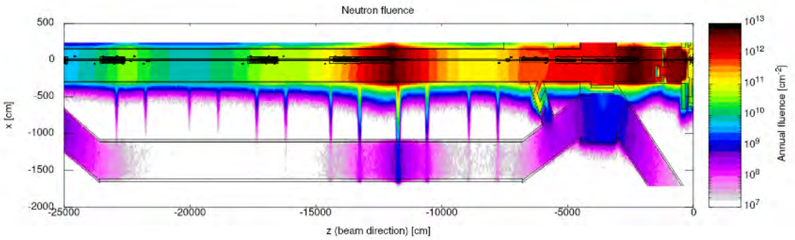

Fig. 11: The neutron fluence in the vicinity of MAPP-1. The top part of the map shows the UGC1 gallery and the bottom map shows the UA83 tunnel.

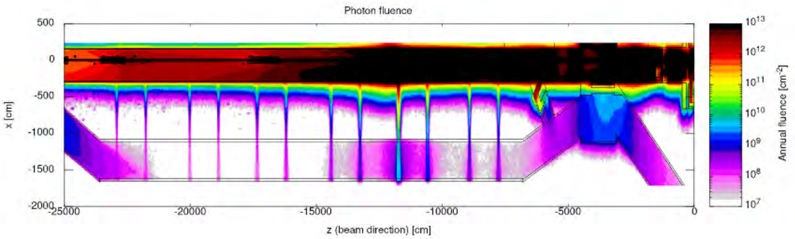

Fig. 12: The photon fluence in the vicinity of MAPP-1. The top part of the map shows the UGC1 gallery and the bottom map shows the UA83 tunnel.

3.1 Beam and Cosmic Backgrounds in the Vicinity of the Outrigger

In the region by the mouth of the ducts in the UA83 tunnel, the beam-induced backgrounds rise substantially, since radiation can travel down the shafts unimpeded. Thus, before we install the outrigger detectors in shafts 3,4 and 5 we will install 2m of shielding in the beam-tunnel side of the shaft. The result of doing this for shafts 4 and 5 are given in Figures 13, and 14 where the peak values obtained in the ducts are shown.

For shaft 3, the 2m of shielding reduces the annual dose by a factor of around 300 from 3 x 10^4 mGy to 10^2 mGy for a luminosity of 10 fb. The thermal neutron fluence is reduced by a factor of over 150 from 10^{11} cm^{2}yr^{-1} to 7 x 10^8 cm^{-2}yr^{-1} and the High Energy Hadron (HEH) flux is attenuated by a factor roughly 10 to 6 x 10^8 cm^{-2}yr^{-1}. For an instantaneous luminosity of 2 x 10^{33} cm^{-2}s^{-1} the estimated photon fluence is diminished from 10^5 cm^{-2}s^{-1} to 3 x 10^2 cm^{-2}s^{-1}. In the case of muons the fluence is reduced by a factor of about 8 to 10 cm^{-2}s^{-1}

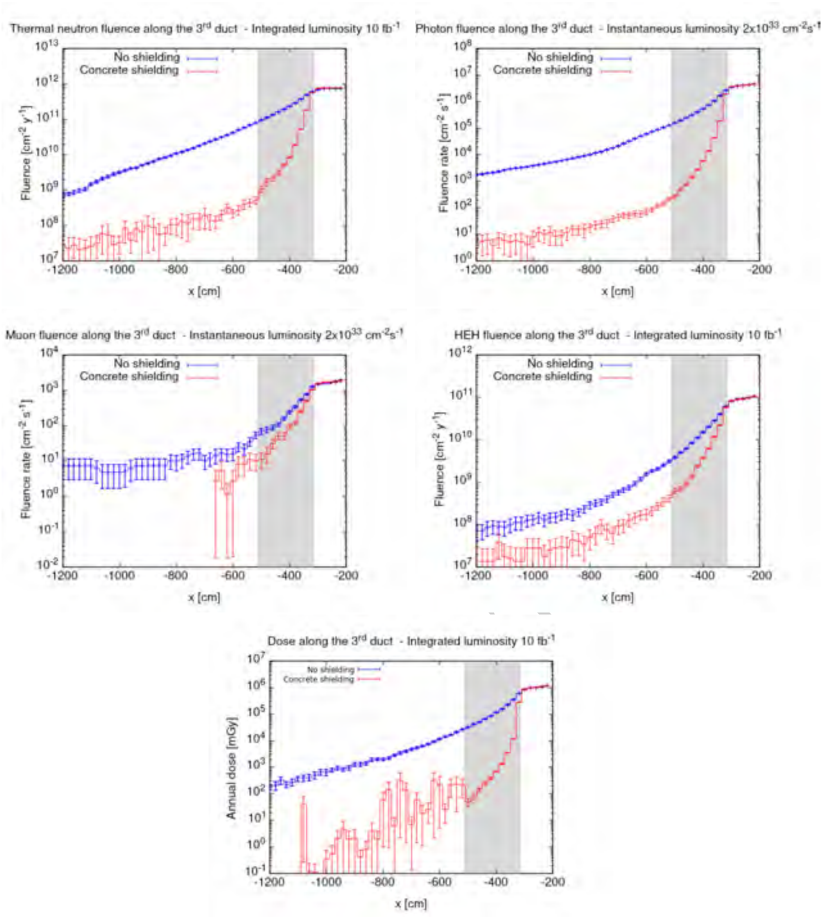

Fig. 13: The radiation levels in the 3rd duct on the UA83 tunnel.

As the TANB absorber is adjacent to the mouth of shaft 4 the beam backgrounds are somewhat higher than in shaft 3. For shaft 4 the 2m of shielding reduces the annual dose by a factor of nearly 300 to 0.1 Gy for a luminosity of 10 fb. The thermal neutron fluence is reduced by a factor of over 200 from 10^{12} cm^2yr^{-1} to 2 x 10^9 cm^2yr^{-1} and the High Energy Hadron (HEH) flux is attenuated by a factor roughly 30 to 10^9 cm^2yr^{-1}. For an instantaneous luminosity of 2 x 10^{33} cm^2s^{-1} the estimated photon fluence is diminished from 10^6 cm^2s^{-1} to 10^3 cm^2s^{-1}. In the case of muons, the fluence is reduced by a factor of 10 to 10 cm^2s^{-1}.

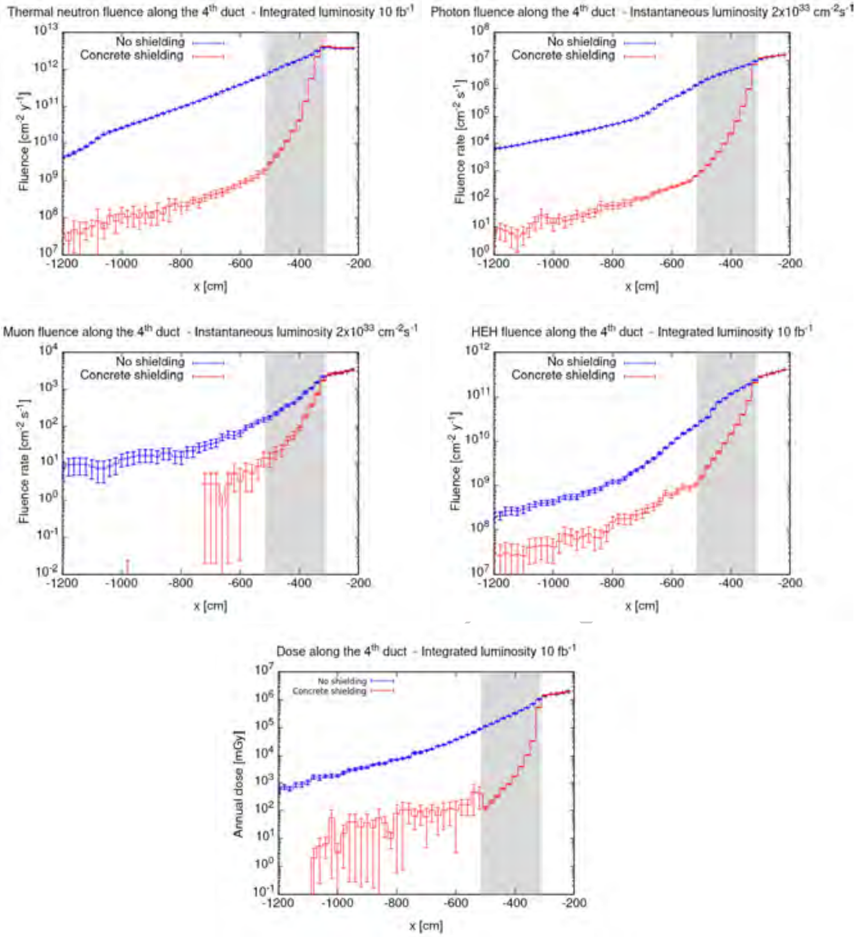

Fig. 14: The radiation levels in the 4th duct on the UA83 tunnel.

4 Construction and Installation of the Outrigger Detector

The detector will be constructed and tested at the University of Alberta. It will then be broken down to its constituent elements, none of which weigh more than 20kg, and then shipped to CERN for installation in the UA83 tunnel. Once situated, the detector and its readout chain will be tested in situ before data taking. T-slot extrusion (45 mm x 45 mm) is used to construct the framework to support the scintillator blocks. In practice, the basic units are assembled into 4 block (shaft 3) and 2 blocks (shafts 3 and 4) substructures for handling and insertion into the shaft. A Gantt chart showing the envisaged construction schedule is given is provided in Figure 15 and Figure 16.

structure.png

Fig. 15: The construction schedule for the Outrigger Detector scintillators.

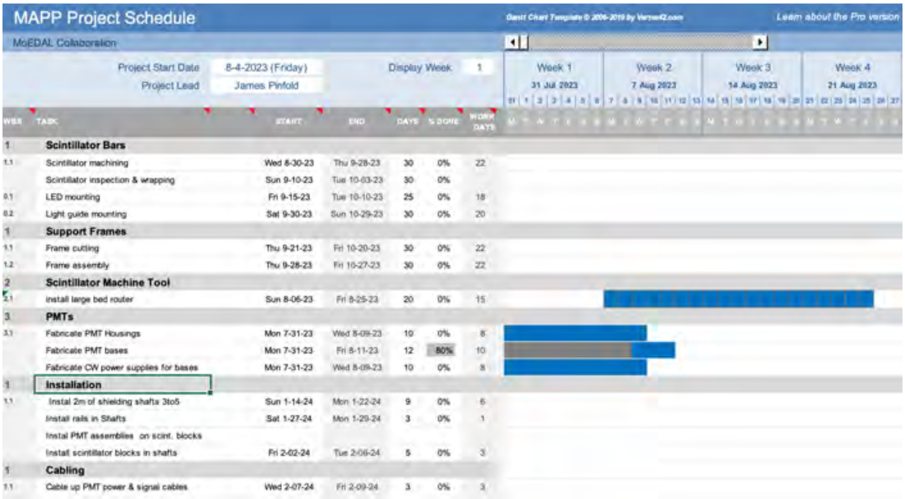

Fig. 16: The construction schedule for the Outrigger Detector PMTs and related technology.

4.1 Installation of Required Infrastructure

The substructures are inserted into the shaft along rails fixed on each side of the shaft. A total of 10 subunits (roughly 20 blocks wide) are installed in each shaft. The total area of plastic seen by particles from the IP as they impinge on shaft 3 is 20 x [30 x 60*Sin 45°] = 2.5 m^2, compared to $\sim$ 1 m^2 for the MAPP-1 detector

The readout of the PMTs as well as the calibration system is connected to the main readout electronics readout rack of the MAPP detector. The electronics readout and calibration system is functionally the same as that of the MAPP-1 detector. The cables carrying LV power and signals to and from the PMTs are housed in the cable rack installed the length of each shaft behind the scintillator blocks. Details of the installed detector are given in Figure 6 and Figure 7.

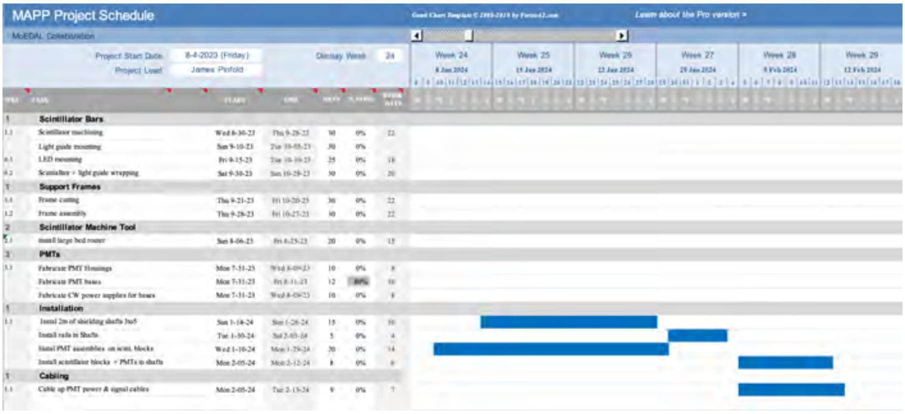

Fig. 17: The installation schedule for the shielding, the installation rails, the cable trays, the Outrigger Detectors with PMTs and cables.

The installation starts with the attachment of the PMTs and light-guides to the scintillator blocks during week in January 2024. Contemporaneously, the shielding will be installed, filling the 2m of ducts 3, 4 and 5 nearest the beam tunnel. After the 'shielding has been installed the rails and cable trays within the ducts will be put in place. Starting at the beginning of February 2024, the scintillator PMT units will be cabled and placed in the ducts using the rails. The installation schedule for the Outrigger Detector is summarised in Figure 17

4.2 Staging and Temporary Storage Area

In order to facilitate the installation and operation of the Outrigger Detector the LHC machine side manager responsible for allocation of surface space in the SBD building agreed that MoEDAL-MAPP Experiment can be temporarily attributed about 20 m^2 of surface space in SBD 2855, as indicated in the photograph in Figure 18. This area will be used as buffer space for short term storage of equipment before transport and installation underground, and for storing light tooling needed for assembly and installation.

5 Safety Matters

The safety issues considered below arise from four sources, those to do with: the UA83 tunnel; the detector itself; and, detector operations.

Fig. 18: The temporary staging area in SBD 2855.

5.1 UA83 Tunnel and Detector Safety Issues

The UA83 tunnel is a full part of the LHC machine infrastructure with access via the PM85 lift directly to the floor of UA83. It has interlock access, smoke detectors, fire alarms and forced ventilation.

The MAPP-mQP and the Outrigger Detector employ conventional detector technology involving scintillator detectors and electronic readout, no gaseous detectors are involved. The safety issues directly related to the MAPP-mCP detector detector are presented in an approved Safety Derogation Request (SDR) [3] and described directly below. The SDR is included in Appendix (A).

The acrylic-based scintillator detector elements of the Outrigger are completely enclosed in three horizontal concrete ducts. The total mass of plastic scintillator in Shaft 3 is 400 kg, with 200kg of scintillator in each of the ducts 4 and 5. The safety sheets for acrylic plastic are included in Appendix (B). Thus the Outrigger detectors are completely surrounded by metres of concrete, except for the opening into the UA83 tunnel. An aluminium flame shield will be placed across the mouth of the opening to completely isolate the detectors.

The MAPP/Outrigger detector electronics rack and MAPP detector are monitored by an IR + Visible light digital camera placed in the vicinity of MAPP in the UA83 tunnel. The Outrigger detectors which do not obtrude into the UA83 tunnel are situated in ducts that will be equipped with smoke and temperature detectors, that are monitored in the same way as the MAPP-1 temperature and smoke sensors.

5.1.1 Safety Issues Related to the Readout Electronics & HV

The readout electronics and power supplies are isolated and deployed up to 30m from the Outrigger Detectors in the electronics racks servicing the MAPP-1 detector. There are no HV cables or HV connectors as there is a "Cockcroft-Walton" type converter in the base of each PMT that converts LV power to HV power for the PMT. The power supplies are low voltage (24V), are current and the temperature limited (turn off when current or temperature goes out of a predetermined range), and provide an alarm signal when current or voltage moves out of some predefined operating window. The MAPP-mQP and Outrigger detector electronics consume only 1800 watts of power.

All cabling is halogen-free according to the provisions in IS23 [3]. The only other heat source in the UA83 gallery arises from the MAPP-mQP detector electronics and amounts to only 1400 watts.

5.2 Safety Issues Relating to Detector Installation

MAPP-1's outrigger detector is designed to be installed in situ from pieces weighing a maximum of approximately 20 kgs each. Thus the whole Outrigger detector can be taken underground using the machine side elevator at IP8. We envisage that a maximum of four people will need to be present in the UA83 gallery for installation of the MAPP Phase-1 detector. MoEDAL-MAPP's installation personnel will, of course, be equipped with all the required safety gear and will operate according to the safety rules and guidelines described in the safety courses that each member of the team will have taken and passed.

5.3 Safety Monitoring After Detector Installation

The MAPP-1 Outrigger detector is readout over ethernet through the same pathways as the MAPP-1 detector. It does not require a team to operate it during data taking. However, it is important that the detector is monitored to ensure safe operation at all times. The safety systems that will be installed to ensure that the detector is operating safely are as follows:

- The power supplies are current limited. In addition, alarm conditions are defined that signal non-standard operating characteristics. The power supplies output and alarm conditions are monitored remotely with a feed supplied to the CERN Control Centre (CCC);
- Three temperature probes will be placed at the end, middle and entrance of each of the three shafts housing the outrigger detector. Alarm conditions are defined that signal if any monitored temperature moves above normal ambient temperature in the UA83 tunnel. The temperature probe outputs and alarm conditions are monitored remotely with a feed supplied to the CCC;
- A smoke detector that can be monitored remotely will be placed within the mouth of each of the ducts containing Outrigger Detectors;

[3] https://edms.cern.ch/document/335745/4

- An IR camera will be installed on site to monitor the whole MAPP-1 detector region. Again, the feed from the camera will be supplied to the CCC.

5.4 MoEDAL-MAPP Safety Organization

The MoEDAL-MAPP safety organization at CERN will be established prior to installation. It will consist of:

- An experimental Safety Officer (EXSO, formerly GLIMOS) as the point of contact for all experimental safety issues and communication with the EP Safety Office. The EXSO for MoEDAL for installation and the first year of running, will be the Technical Coordinator, Richard Soluk;
- Both the EXSO and the MoEDAL-MAPP Spokesperson will be available for urgent safety interventions required during the detector installation;
- All the activities of installation will be declared via IMPACT request and analyzed via the usual work package analysis and VIC (Visite Inspection Commune) procedures ;
- The MoEDAL-MAPP safety files will be created on EP safety office EDMS and shared with the LHCb LEXGLIMOS.

6 Organization of Construction, Installation and Running of the Detector

The two bulleted lists below describe the basic organization of the construction and installation of the Phase-1 MAPP-mCP detector:

- Project Managers:
  - MoEDAL Spokesperson - James Pinfold;
  - MoEDAL Technical Coordinator - Richard Soluk;
  - Chief engineer - Mitchel Baker;
  - Chief electronics engineer +Trigger and DAQ coordinator - Paul Davis;
  - CERN based administrator - Veronique Wedlake;
  - CERN based liaison with Machine - Francois Butin;
  - EXSO(GLIMOS) - Richard Soluk; Safety Officer - Richard Soluk
- Installation Crew
  - Richard Soluk - Crew leader and responsible for mechanics installation;
  - Paul Davis - Readout electronics, power supplies and FPGA-based trigger;
  - Aditya Upreti - General team member to assist in all aspects of installation;
  - Emanuela Musumeci - General team member to assist in all aspects of installation
  - Michael Staelens - General team member to assist in all aspects of installation
  - Mitch Kelly - General team member to assist in all aspects of installation

- Phd-student/Post Doctoral student 1 - General team member to assist in all aspect of installation;
- Phd-student/Post Doctoral student 2 - General team member to assist in all aspect of installation.

7 Maintenance and Operation of the Outrigger Detectors for MAPP-1 During Run-3

The MAPP-1 and Outrigger detector will be read out via ethernet during the run to large-scale onsite disk storage at CERN. The UA83 gallery is not accessible during LHC running periods. In the event of a failure or malfunction of the Outrigger Detector, we will not be able to effect repair until we have a TS, or a YETS in which access to the UA83 tunnel is possible. Typically, there are a few Technical Stops (TSs) within the year besides the YETS.

We could continue running with the failure of a large fraction of the readout channels although understandably this would compromise the physics performance of the detector. In order to reduce the risk of shutdown of data taking during the run we have included in our electronics design a redundant power supply system and a redundant DAQ computer, to ensure robust operation of the overall detector.

In order to continue data taking in the event of a disruption of the ethernet connection, the DAQ server will have 60TB of local disk storage. Data will be written to this disk until the ethernet connection is re-established. During normal running the data rate will be below 0.5 TB/day allowing an extended running period without exporting data to remote storage. Initially, the fewest possible restriction will be applied to the trigger, and storage write speeds will limit the data rate.

The MAPP detector is designed to be operated remotely and to shut down if any MAPP-1 or Outrigger Detector power supply draws more than a set maximum current. Nevertheless, the MAPP-1 and Outrigger detectors must be monitored 24/7 by personnel based on site primarily for safety purposes - as described in Subsection 5.4. This team would be enhanced by an average of 0.5 FTE person, formed from MoEDAL-MAPP collaboration members who are visiting CERN and have the required safety training. For planned upgrades or maintenance during running periods, we will call on manpower resources described in Subsection 6.

7.1 The Outrigger Detector Control Centre

The base of operations of the MAPP detector is the MAPP Control Centre (MCC) in Bat. 17 R-007, the location of which is shown in Figure 19. MAPP's CERN-based operators have access through their on-call cell phones to the monitoring and alarm system as well as simple controls that allow them to turn off the power and alert the CCC. The on-call MAPP operator, the off-duty operator, and the Technical Coordinator + Spokesperson are also connected to this system at all times via cellphone. During the day the on-call MAPP-1

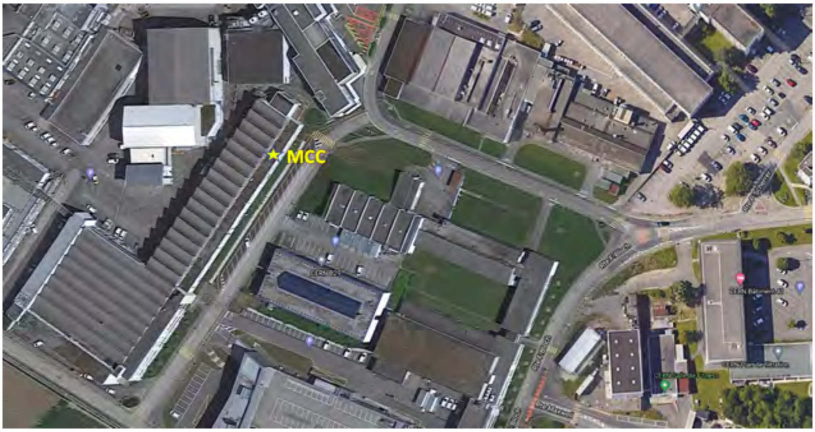

Fig. 19: The location of the MAPP-1 and Outrigger Detector Control Room (Bat. 17 R-007).

Outrigger operator will usually sit in the control room. During the evening and night, the on-call will be connected by cell phone to the MAPP-1 and Outrigger control and monitoring services. The on-call cell phone will be switched on at all times.

8 Funding Plans for the MoEDAL-MAPP Phase-1 Installation

The MAPP-1 Outrigger detector project has been made possible by contributions of equipment from other experiments, including long-term loans of scintillator from EXO-200 and surplus HZC PMTs from a cancelled astroparticle physics experiment. We will use the same electronic readout and calibration technology utilized by MAPP-1, including electronic readout, DAQ, calibration and safety systems. The funding needed for extra readout boards, PMT bases, LED calibration units and power supplies will; be provided from MoEDAL-MAPP M&O funds, MoEDAL-MAPP-1's NSERC Discovery Grant; and, contributions from the UofA DUP funds. All required funding for the project is now in place.

Regarding manpower, our project electronics engineer, mechanical engineer and detector technologist are funded by our existing NSERC MRS grant. We have sufficient funds in hand to deploy the Outrigger detector (as described above) to take data in Run-3.

9 Physics Issues

In order to fully understand the sensitivity of the MoEDAL-MAPP detector to we are performing studies of a number of relevant physics benchmarks. Examples of initial benchmark studies are presented below. To complete these physics studies we need to fully and accurately simulate: the detector and its response; the passage of primary and secondary particles through the intervening infrastructure; and, the transport of cosmic ray particles through the 105 m overburden. The complete Simulation package UA83-MAPP-MoEDAL Arena (SUMMA) is discussed below.

9.1 The Full Simulation of the UA83, MoEDAL, MAPP-mCP Arena (SUMMA)

The previous version of SUMMA, with the MAPP-mCP detector deployed in the UGC1 region, was nearing completion in Spring of 2021 when the decision was made to move MAPP's location to the UA83 tunnel. The move required an extensive update to the SUMMA code to take into account the MAPP-mCP's new final position approximately 100m away (UA83) from the IP. Additionally, the modelling of the intervening infrastructure had to be completely redone. However, SUMMA's existing cosmic ray simulation module did not require extensive updates.

The SUMMA simulation is derived from: the final CAD drawings of the MAPP-mCP detector; accurate CAD drawings of the machine infrastructure; and, the existing model of cosmic ray transport through the overburden. In all, the simulation involves over 2500 elements. The SUMMA code will be ready for use in mid-December 2021.

The Physics Processes included in SUMMA, are:

- Primary Interaction and secondary particles, factory lists :
  - FTFP_Bert model of hadronic showers
  - QGSP_BERT_HP for neutron fluxes
- Transportation and Decay;
- Electromagnetic Interactions.
  - Gamma conversion, Compton scattering, photo-electric effect for gammas;
  - Multiple scattering, ionization, bremsstrahlung for electrons and annihilation for a positron;
  - Multiple scattering, ionization, bremsstrahlung and pair production for muons;
  - Multiple scattering and ionization for other particles.
- Scintillation processes
  - Scintillation and Cerenkov for particles;
  - Absorption, Rayleigh scattering, Mie scattering and boundary processes for optical photons.

The SUMMA ionization energy loss calculation for milli-charged particles is based on the approach adopted in Reference [5]

9.2 Mini-Charged Particles from Dark QED - a Physics Benchmark

In an initial study of the sensitivity of the MAPP-1 Outrigger detector to mCPs. We here consider a class of Feebly Interacting Particle (FIP) that has a mini-charge (mCP) as small as $10^{-3}e$, or lower. A common scenario is from a Dark Sector model where one considers a mCP coupled through a very light kinetically mixed dark photon [6][7]. Although the mCP does not carry SM electroweak quantum numbers, it behaves as a particle with a tiny electric charge. The Feynman diagrams for the most important production mechanism of mCPs at the LHC are shown in Figure 20.

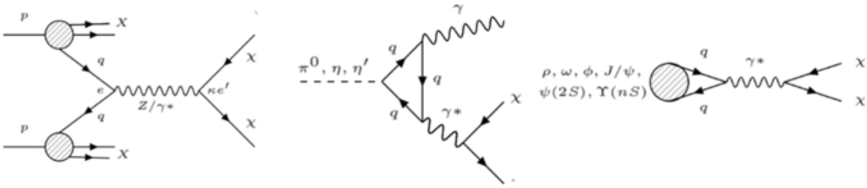

Fig. 20: The Feynman diagrams for the most important production mechanism of mCPs at the LHC: (left) DY production; (middle) Dalitz decays of pseudoscalar mesons; and, (right) direct decays of vector mesons.

The DY process provides the main production channel for GeV-range mCPs at the LHC. The sensitivity of the MAPP-mCP detector deployed at UA83 to mini-charged particles produced in this way is shown in Figure 21 The sensitivity of the MAPP-mCP detector deployed at UA83 to mini-charged particles produced by DY production is shown in Figure 21. The Outrigger Detectors provide a clear improvement over the whole higher mass region ofo 1 GeV/c^2 and above.

If we include all of the processes shown in Figure 20 the sensitivity of MAPP-1 for masses below ofo 1GeV/c^2 improves considerably and in a very competitive way. However, we should note that the efficiency of the MAPP-1 and Outrigger Detectors is assumed to be 100%, with zero background. The milliQan analysis on the other hand has considered detector efficiency and backgrounds. The final MAPP-1 efficiency and backgrounds

Backgrounds

A potential source of background mentioned previously is the dark count from the PMT. For the HZC-photonics, the dark count rate is typically 600 cps. Considering the mCP trigger, that consists of requiring an mCP signal in 4 collinear blocks in coincidence, with a trigger window of 25 ns and a beam crossing rate of 40 MHZ, we would expect a trigger rate due to the dark count rate in the PMTs, of roughly 0.003, in a data-taking year of 1.5×10^7 s.

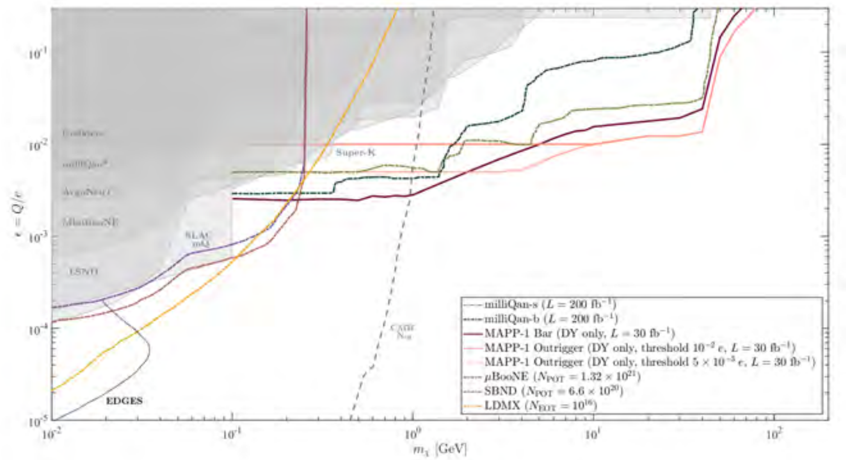

Fig. 21: Direct bounds from accelerator-based searches and indirect bounds from the effective number of neutrinos from Planck are shown. The projected sensitivity for mCPs, for models with a massless dark photon, are presented for milliQan (for the slab (s) and bar (b) detectors and MAPP-mCP (for the MAPP-mCP bar (B) and Outrigger (O) detectors) at Run-3. The existing bounds are provided for approved detectors or detectors in the process of approval [8].

The MAPP-mCP detector is protected from cosmic ray backgrounds by a 105 m overburden. MilliQan, by comparison, is deployed near to the CMS detector at a depth of 73m. The cosmic ray background expected in the MAPP-mCP detector has been assessed by the MoEDAL-MAPP simulation group to be $(4.04 \pm 0.06) \times 10^{-5}$ cm^{-2} s^{-1}. This amounts to about 2 muons/s incident of the top of the MAPP-mCP veto detector, with area ~ 4.5 m^2. This rate is inconsistent with measurements taken in the UGC1 gallery in 2018. Considering the trigger requirement for mCPs and the high efficiency of the MAPP-mCP veto system the background from uncorrelated CR muons is expected to be negligible.

The most important source of background is thought to be due to cosmic ray events with high muon multiplicity where a number of muons penetrate underground together, This has been observed, for example, by the ALICE [10] TPC with effective CR muon detection area of 17m^2 and 28 m rock overburden, where the corresponding figures for the MAPP-mCP detector at 4.4 m^2 and 105 m. The concern is that a number of particles could impinge on the detector together increasing the probability of satisfying the mCP trigger conditions. However, the greater the multiplicity of muons impinging on the MAPP-mCP detector region, the greater the chance one of these muons would VETO the event. There are several additional factors that act to reduce this potential source of background:

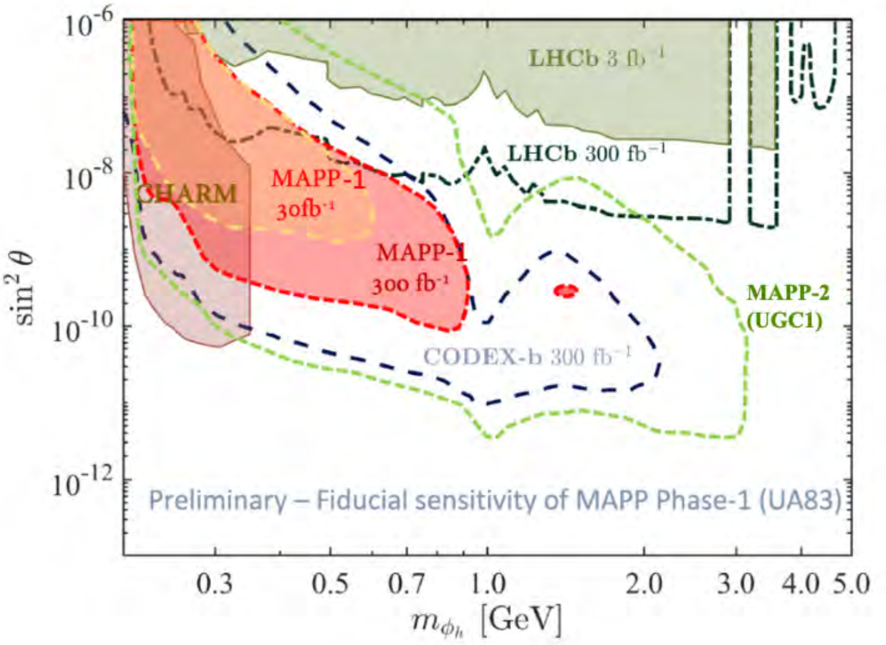

Fig. 22: 95% C.L. exclusion bounds on dark Higgs bosons produced at the HL-LHC at a center-of-mass energy of $\sqrt{s} = 14$ TeV for the MAPP-2 detector (considering a total integrated luminosity of $\mathrm{L} = 3\ \mathrm{ab}^{?1}$), compared to previous results obtained for MAPP-1 and CODEX-b [9]

r

- The rate of these showers is very small compared to the rate of single uncorrelated particles given above. For example, the ALICE data shows over six orders of magnitude fall in the number of events with a multiplicity of 20 muons compared to just a few muons;
- For cosmic ray muons from above or below to reach a bar and give even a small mCP signal the charged CR particle would normally need to cross two VETO counters which have an efficiency better than 99.7% and "clip" a bar. This would need to happen four times in four contiguous bars within the trigger time window, without hits from other CR muons in the shower registering in the VETO system;
- The rate of horizontal cosmic rays is greatly suppressed compared to the downward flux. If horizontal cosmic ray muons do reach the MAPP detector they must pass through four vertical veto walls of thickness 2.5 cm that are placed in front of MAPP and between each MAPP section, and also the back wall of the cosmic ray VETO detector of thickness 1 cm, to satisfy the mCP trigger;
- Neutrons associated with the muon shower can evade the VETO system and cause, for example, a nuclear recoil that can give rise to a small signal in a

bar. This would need to happen in four contiguous bars within the trigger time window. At the same time, the accompanying charged particles in the shower would have to miss the VETO system.

As stated above in Section 2 we can monitor the VETO system, with collisions-off and collisions-on, for any penetration of the VETO system. If necessary we can utilize the outer layer of scintillator bars in MAPP-mCP detector as an additional VETO system.

Importantly, can study non-beam-related background sources experimentally by running in the winter while the beam is off. In this way, we can directly register background events that mimic a signal. These runs can be used to hone our estimates of non-beam-related backgrounds.

10 Conclusion

The MAPP-1 Outrigger Detector is designed to enhance the acceptance above a mCP mass of approximately 5 GeV/c^2 as shown in Figure 21 for the standard benchmark process [6][7] of DY production of mCP pairs. The MAPP-mCP detector and Outrigger Detector is very competitive with the milliQan detector [11] that will also be deployed for Run-3 and covers a different pseudo-rapidity range. In the event of the discovery of a mini-charged particle by MAPP-mCP and milliQan, a signal seen in two different detectors with their different systematics would provide the necessary confirmation of a discovery. Indeed, the use of multiple experiments to provide verification for important experimental findings has been adopted at LEP (ALEPH, DELPHI, L3 and OPAL) as well as the LHC (ATLAS and CMS).

Additionally, although MAPP-1 is designed primarily to detect feebly ionizing particles such as mCPs, its has some but useful sensitivity for neutral LLPs, s shown in Figure 22. It could in some circumstances provide a confirmation of a signal observed by FASER [12] or vica versa. We are currently investigating the use of the Outrigger Detectors to enhance the sensitivity of MAPP-1 to neutral LLPs.

References

The Bibliography

[1] J. L. Pinfold, The MoEDAL Collaboration, “The MAPP Technical Proposal, ” to be published in EPJ-ST.

[2] D. van Eijk, J. Dorant, C.Wendt, and A.Karle, “Characterization of the HZC Photonics XP82B20D and XP1805D Photomultiplier Tubes for Low-Temperature Applications,” arXiv:1904.11897v2 [physics.ins-det] 23 Jun 2019.

[3] M. Tanabashi et al. (Particle Data Group), Review of Particle Physics,” Phys. Rev. D98, 030001 (2018).

[4] 2631839 v.1 ”Derogation to IS41 MoEDAL MAPP Experiment UA83” by Fabio CORSANEGO in status: Released Link: https://edms.cern.ch/document/2631839/1/approvalAndComments

[5] K. J. Kelly and Y.-D. Tsai, “Proton Fixed-Target Scintillation Experiment to Search for Minicharged Particles,” arXiv:1812.03998v2 [hep-ph] 14 Dec 2018.

[6] B. Holdom, “Two U(1)’s and ϵ charge shifts”, Phys. Lett. B 166, p196-198 (1986).

[7] A. Haas, C. s. Hill, E. Izaguirre, I. Yavin,“Looking for milli-charge particles with a new experiment at the LHC”, Phys. Lett. B746, p117-120 (2015).

[8] To be provided.

[9] Michael Staelens, “Physics From Beyond the Standard Model: Exotic Matter Searches at the LHC with the MoEDAL-MAPP Experiment,” PhD Thesis, University of Alberta, 2021.

[10] J. Adam et al., ALICE Collaboration, “Study of cosmic ray events with high muon multiplicity using the ALICE detector at the CERN Large Hadron Collider,” Journal of Cosmology and Astroparticle Physics 2016 (2016) 32.

[11] A. Ball et al., “Sensitivity to millicharged particles in future proton-proton collisions at the LHC with the milliQan detector,” milliQan Collaboration, Phys. Rev .D 104 3, 032002 (2021).

[12] A.Ariga et al., FASER Collaboration, “FASER’s physics reach for long-lived particles”, Phys. Rev. D99 no.9, 095011 (2019).

Appendix A Safety Derogation Request

HSE
Occupational Health & Safety
and Environmental Protection Unit

Safety Derogation Request Form		
Date	**Requested by**	**Dpt/Group**
27 août 2021	MoEDAL- MAPP Experiment EP Safety Office	EP

DESCRIPTION OF THE REQUEST

Location / Project :
UA83

Regulation related to the derogation:
Plastic materials needed for the MoEDAL Detector are not conforming to CERN IS41, and specifically needed due to their physical properties.

Brief description of the Detector :
The MAPP detector is comprised of 400 x (10 cm x 10 cm x 75 cm) scintillator bars, wrapped in Tyvek and then black tape. Each bar is connected via a short light guide to a 3-inch PMT. The bars are arranged in 4 sections, each with 100 bars with overall sensitive area of 1m^2. The scintillator bars (NUVIA polystyrene based scintillator) in each section are held in a square array by three support grids made of High-Density Polyethylene (HDPE). A drawing of one of the basic HDPE support grids is shown in Figure 1. The grid separates the bars one from the other by 5m to 7 mm. The air fills the interstices between the scintillator bars.

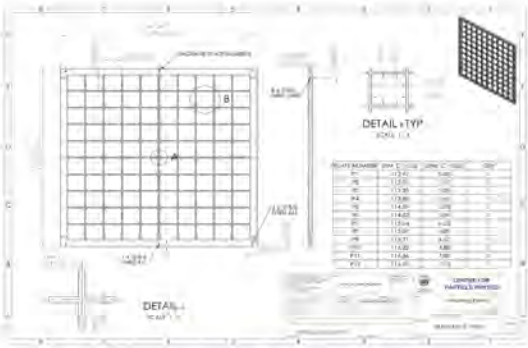

Figure 1: The drawing of one of 12 HDPE support grids of the MAPP-mQP detector

The weight of the scintillator in each section is supported by an aluminium T-bar support structure and a 0.5 cm aluminium plate that forms the base of each section. Additionally, each section is protected from the other by the lead-scintillator radiator plane that includes 2 x 1 mm of aluminium sheet and 5 x 2mm layers of lead. The active detector is completely encapsulated in VETO detectors comprised of 1 cm thick acrylic scintillator (Eljen-200 PVT based scintillator). with area roughly 30m^2. The above arrangement is shown in Figure 2. The support structures and metal plate elements are shown in blue. The HDPS support grids and metal support structures are further emphasized in Figure 3.

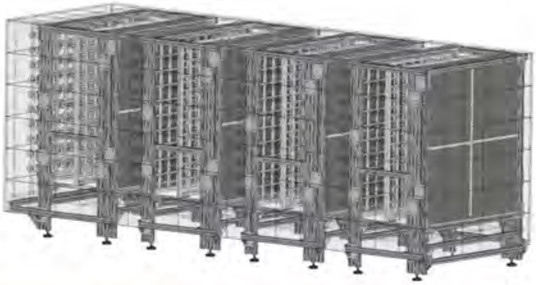

Figure 2: The basic structures of the MAPP-mQP with the outer VETO layer and the support structures emphasized

Figure 3 The basic structures of the MAPP-mQP without the outer VETO layer the support structures emphasized.

The MAPP detector and VETO layer are completely enclosed in the MAPP-mQP flame shield as shown in Figure 3. The size of the shield is roughly 1.3 x 1.5 x 4m. The flame-shield is fabricated out of 1mm thick aluminium sheet and has a total area of ~30 m^2. The aluminium encloses the plastic scintillator completely. There is no break in the flame shield for cable exit. The cables exit via a patch panel.

Figure 4 The flame shield around the MAPP-mQP detector

In order to provide a hermetic environment all joints in the flame shield are sealed using heavy duty aluminium tape shown in Figure 5. Any fires within the flame shield volume would be suppressed due to lack of oxygen. The slight electrical heating arising from the PMT bases within the volume of the flame shield – the only electrical elements in the region - amounts to a few hundred Watts that is dissipated by conduction and radiation from the flame shield surface

The foreseen location in UA83 is shown in Figure 5 and Figure 6 here below.

Figure 5: Proposed location in UL83

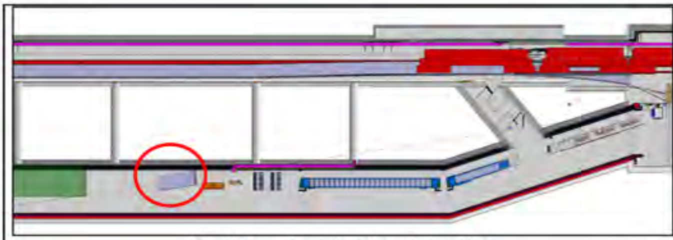

Figure 6: Proposed layout of the MAPP-mQP setup in UA83.

Further details on the materials used and other cases of applications at CERN are available in the document: **"Information Relating to Safety of the MAPP Detector With Respect to Flammability"** From J.Pinfold, available in this same EDMS node.

Further details on the installation in the UA83 are given in the ECR "LHC-X8MAPP-EC-0001 MoEDAL MAPP mQP detector in UA83" (EDMS 2617044).

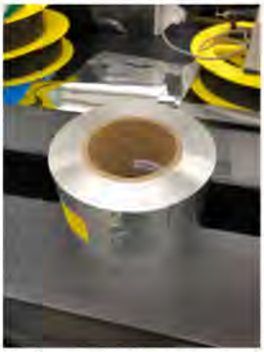

Figure 7 Heavy duty aluminium tape (0.25 mm thick), used to seal the flame shield

Gap compared with the reference regulation

Description:

Materials specifically needed for the MoEDAL Detector in virtue of their physical properties are not conforming to CERN IS 41:

Polystyrene (PS)

https://edms.cern.ch/ui/file/2631839/1/Polysyrene_Material_Data_Sheet-AMCRYS.pdf

High Density Polyethylene (HDPE)
(https://edms.cern.ch/ui/file/2631839/1/Recycled_HDPE_Material_Safety_Data_Sheet.pdf)

Polyvinyl Toluene (PVT)
https://edms.cern.ch/ui/file/2631839/1/EJ-200-SDS_PVT_Material_Safety_Data_Sheet.pdf

Cause and justification of the gap:
PS is required for the operation of scintillation detectors in order to perform physics in MoEDAL Experiment

Quantity : (kg or m^3)	**Dimensions :** (length, width, diameter, thickness)
3,000 kgs of PS HDPE 326kg PVT 406kg	PS: 10 x 10 x 75 cm / 100 units x 4 HDPE: support spacers grids --various measures described in Figure 1 PVT: set of plates, 1cm thick, total 30m²

Ignition sources:
Low Voltage circuitry
Distance to the nearest external powered system:
An uninterruptible power supply, part of other LHC equipment, is at a distance ~1.5 m

Are there other previous derogation requests for the equipment/building/installation…?
Not for this installation (A previous derogation has been made for MoEDAL in UX85 EDMS 893563).

What are the alternatives that have been investigated and why were they not put into place ?
The scintillators for the detector are housed within a flame-resistant metal casing, to prevent the propagation of fire. This mitigation is considered in the context of the derogation request required from HSE. This measure is integral to the detector and does not require any external mitigation measures.
The material properties of PS are required for scintillator detectors of this type, no other alternative is possible.

Documents provided by the requestor:
Click or tap here to enter text.

APPLICABLE SAFETY DOMAIN

(a single domain per derogation)

☐ Mechanical (pressure, lifting, machines, HVAC…) ☐ Cryogenics ☐ Structural, civil engineering ☒ Fire Safety ☐ Chemical	☐ Workplace ☐ Flammable gas ☐ ODH ☐ Electrical ☐ Noise	☐ Non-ionising radiation ☐ Environmental protection ☐ Others: Click or tap here to enter text.

SPECIALIST OPINION

Specialist:
Fabio CORSANEGO HSE-OHS-IB Jonathan Gulley HSE-OHS-PE

Specialist opinion:
Acceptable with the conditions agreed here below

Compensatory measures defined in collaboration with the requestor:

safeguards: hardware/software interlocks

power supplies are low voltage (24V), are current and temperature limited (turn off when current or temperature goes out of range) and provide an alarm signal when current or voltage moves out of some predefined *operating window*.

handover of alarms generated by the system

Three types of warning/alarm information will be provided to the CCC:

1) The current/voltage and temperature readings/alarms from the power supplies,
2) The hermetic metal flame shield is monitored by temperature sensors placed on the outside of the shield. The output of these temperature sensors will also be provided to the CCC,
3) There is a plan (not yet confirmed) to monitor the detectors + electronics with an IR camera whose output is provided to the CCC.

Other safeguards:

1) The power supplies, readout electronics and other non MoEDAL live equipment present in UA83 are separated by a distance of 1.5 m from the detector,
2) The only entities that use power in the detector volume are PMT bases. Power supplied to the bases is LV and only stopped up in the base,
3) The detector volume is completely encased in a hermetic (sealed to exclude air movement) flame shield. Cables enter the volume via a patch panel. Metal planes separate each of the four compartments of the detector. A strong metal plate forms the base of the scintillator bar compartments.

Conditions for the validity of the derogation :

☐ Temporary derogation - expiry date : Click or tap to enter a date.
☒ Permanent derogation

Description of the conditions for retaining validity:
Observance of the conditions defined in this document

Documents applicable to the reply:

TRACEABILITY

Reference and version EDMS : https://edms.cern.ch/document/2631839/1

STATUS OF THE DEROGATION

See EDMS

Appendix B Safety Data Sheet for Acrylic Plastic

Acrylite Acrylic Material Safety Data Sheet

1. Chemical Product and Company Identification

ACRYLITE® FF Acrylic Sheet

Supplier:
A & C Plastics, Inc.
6135 Northdale
Houston, TX 77087-5095

Product Information Number	1-207-490-4242
24 Hour Emergency Number, CHEMTREC	1-800-424-9300

® is a registered trademark

Product Use: building glazing, light advertising, furniture, trade-fair booth design, displays, decoration, Industrial Use

---

2. Composition/Information on Ingredients

This material is classified as not hazardous under OSHA regulations.

Ingredients	CAS Reg. No.	Weight %
acrylic copolymer	trade secret	100

NJTSR # 56705700001-6897 P

See Section 8, Exposure Controls/Personal Protection

---

3. Hazards Identification

Emergency Overview

Color:	colorless or colored
Appearance:	solid in various forms
Odor:	odorless

Under normal conditions of use, this product is not expected to create any unusual industrial hazards.

Primary Routes of Exposure
Eye contact (if exposed to chips)

Potential Health Effects

Inhalation
No hazard expected in normal use.

Eye Contact
No hazard expected in normal use.
Material can cause the following:
- mechanical irritation

A&C PLASTICS, INC.
Service. It's what we deliver.

Pg 1

Acrylite Acrylic Material Safety Data Sheet

Skin Contact
Material can cause the following:
- cuts (when using cut sheets)

Ingestion
No hazard expected in normal use.

Potential Environmental Effects
See SECTION 12, Ecological Information

---

4. First Aid Measures

First Aid Procedures

Inhalation
No specific treatment is necessary since this material is not likely to be hazardous by inhalation

Eye Contact
If mechanical irritation occurs flush eyes thoroughly with a large amount of water, consult a physician if irritation persists. (possible during machining processes)

Skin Contact
No specific treatment is necessary since this material is not likely to be hazardous.

Ingestion
Ingestion is not considered a potential route of exposure.

---

5. Fire-Fighting Measures

Flash point	> 250 °C (ASTM D1929-68) > 482 °F (ASTM D1929-68)
Autoignition Temperature	> 400 °C (ASTM D1929-68) > 752 °F (ASTM D1929-68)
Lower explosion limit	not applicable
Upper explosion limit	not applicable
OSHA Flammability Classification	none

Other Flammable Properties
Use water spray to cool containers exposed to fire.

Extinguishing Media
Use the following extinguishing media when fighting fires involving this material:
water spray - foam - dry chemical - carbon dioxide

Fire Fighting Procedures
As in any fire, wear self-contained breathing apparatus pressure-demand, MSHA/NIOSH (approved or equivalent) and full protective gear.

A&C PLASTICS, INC
Service. It's what we deliver.

Acrylite Acrylic Material Safety Data Sheet

6. Accidental Release Measures

Procedures

Collect material and place in a disposal container. Obey relevant local, state, provincial and federal laws and regulations.

See Material Safety Data Sheet section 8, Exposure Controls/Personal Protection.

---

7. Handling and Storage

Handling

During thermal processing and/or machining local exhaust ventilation at processing machines is necessary.

Storage

Storage: dry.

---

8. Exposure Controls/Personal Protection

Exposure Limit Information

ACRYLIC COPOLYMER

trade secret

No Occupational Exposure Values established (ACGIH, OSHA, Canada and Mexico).

Engineering Controls (Ventilation)

If use operations generate dust, use adequate ventilation.

Respiratory Protection

A respiratory protection program meeting OSHA 1910.134 and ANSI Z88.2 requirements must be followed whenever workplace conditions warrant a respirator's use.

Eye Protection

goggles for machining operations

Hand Protection

protective gloves against mechanical risks

Other Protective Equipment

To identify additional Personal Protective Equipment (PPE) requirements, it is recommended that a hazard assessment in accordance with the OSHA PPE Standard (29CFR1910.132) be conducted before using this product.

---

9. Physical and Chemical Properties

Appearance	colorless or colored
Physical state	solid in various forms
Odor	odorless
Flash point	> 250 °C (ASTM D1929-68) > 482 °F (ASTM D1929-68)
pH-value	not applicable

Service. It's what we deliver.

Acrylite Acrylic Material Safety Data Sheet

Viscosity (dynamic)	not applicable
Specific gravity (water = 1)	1.19 g/cm3 at 20 °C / 68 °F
Vapor density (air = 1)	not applicable
Vapor pressure	not applicable
Softening Temperature	approx. 102 °C / 216 °F
Boiling Temperature	not applicable
Solubility in water	insoluble
n-Octanol/water partition coefficient	not applicable
Evaporation rate	not applicable
Odor threshold	not available
Further information	none

See Section 5, Fire Fighting Measures

10. Stability and Reactivity

Stability
This product is stable under normal storage conditions.

Conditions To Avoid
This material is considered stable.

Incompatibility With Other Materials
Oxidizing agents. No known incompatibility with other materials.

Hazardous Decomposition Products
In case of thermal decomposition, combustible vapours are formed, which are irritating to eyes and respiratory system, mainly consisting of: methyl methacrylate

Hazardous Polymerization
Product will not undergo polymerization.

11. Toxicological Information

Further Information on Toxicology
The product has not been tested toxicologically. When handled and used as directed the product will not cause hazardous effects to health according to studies on similar products and practical experience.

12. Ecological Information

Information on Elimination (Persistence and Degradability)

Ecotoxicological Effect

Further Information on Ecology
The product has not been tested eco toxicologically.
On the basis of the products consistency as well as its low water solubility a bio availability is unlikely.Studies on products with similar composition confirm this assumption.

Acrylite Acrylic Material Safety Data Sheet

13. Disposal Considerations

Procedures

Waste must be disposed of in accordance with federal, state and local regulations. Incineration is the preferred method. A & C Plastics encourages the recycle, recovery and reuse of materials, where permitted, as an alternate to disposal as a waste.

---

14. Transport Information

Further information

Not subject to the regulations on dangerous goods.

---

15. Regulatory Information

INVENTORY INFORMATION

EINECS (EU)	listed or exempted
TSCA (USA)	listed or exempted
DSL (CDN)	listed or exempted

US FEDERAL REGULATORY INFORMATION

Component / CASRN	TPQ [lbs]	CERCLARQ[lbs] (40CFR302.4)	SARA 302 List of EHS	SARA 313 (40CFR372)	TSCA 12b
NONE					

COMPONENT CLASSIFICATION UNDER CLEAN AIR ACT SECTION 112

Component / CASRN	Weight %	HAP	EHAP
NONE			

PRODUCT CLASSIFICATION UNDER SECTION 311/312 OF SARA (40CFR370)

NONE

US STATE REGULATORY INFORMATION

Component / CASRN	New Jersey RTK	Pennsylvania RTK	Massachusetts RTK	California Proposition 65 Cancer	California Proposition 65 Reproductive
acrylic polymer / trade secret	NO	NO	NO	NO	NO

This product contains (a) chemical(s) known to the State of California to cause cancer and birth defects or other reproductive harm.

Acrylite Acrylic Material Safety Data Sheet

CANADIAN REGULATION

This product has been classified in accordance with the hazard criteria of the Controlled Products Regulation and the MSDS contains all information required by the Controlled Products Regulations.

This is a non-controlled product.
WHMIS: NO

Component / CASRN	NPRI
NONE	

16. Other Information

	Health	Flammability	Physical Hazard
HMIS-Ratings	0	1	0
NFPA-Ratings	0	1	0

HMIS Hazard Ratings	NFPA Hazard Ratings
4 = severe	4 = extreme
3 = serious	3 = high
2 = moderate	2 = moderate
1 = slight	1 = slight
0 = minimal	0 = insignificant
N = no rating for powders	N = no rating for powders
* = chronic health hazard	

This MSDS was prepared in accordance with ANSI Z400.1-1998.

Places marked by || have been amended from the last version